

See discussions, stats, and author profiles for this publication at: <https://www.researchgate.net/publication/263946086>

# Subphthalocyanines as Light-Harvesting Electron Donor and Electron Acceptor in Artificial Photosynthetic Systems

ARTICLE *in* THE JOURNAL OF PHYSICAL CHEMISTRY C · SEPTEMBER 2012

Impact Factor: 4.77 · DOI: 10.1021/jp3066103

---

CITATIONS

9

---

READS

23

5 AUTHORS, INCLUDING:



Mohamed E El-Khouly

Kafrelsheikh University

129 PUBLICATIONS 3,162 CITATIONS

SEE PROFILE



Jong-Hyung Kim

Ajou University

8 PUBLICATIONS 72 CITATIONS

SEE PROFILE

# Subphthalocyanines as Light-Harvesting Electron Donor and Electron Acceptor in Artificial Photosynthetic Systems

Mohamed E. El-Khouly,<sup>\*,†,‡</sup> Jong-Hyung Kim,<sup>§</sup> Jung-Hoon Kim,<sup>§</sup> Kwang-Yol Kay,<sup>\*,§</sup> and Shunichi Fukuzumi<sup>\*,†,⊥</sup>

<sup>†</sup>Department of Material and Life Science, Graduate School of Engineering, Osaka University, ALCA, Japan Science and Technology Agency (JST), Suita, Osaka 565-0871, Japan

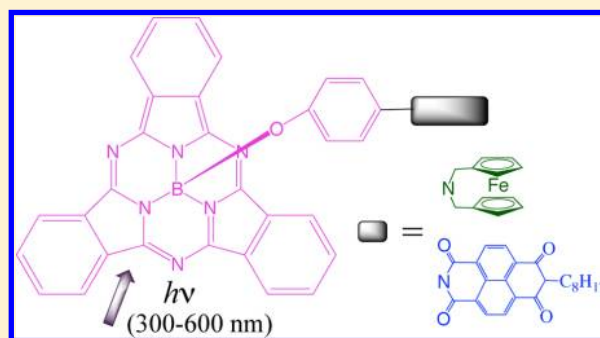
<sup>‡</sup>Department of Chemistry, Faculty of Science, Kafr ElSheikh University, Kafr ElSheikh, Egypt

<sup>§</sup>Department of Molecular Science and Technology, Ajou University, Suwon 443-749, Korea

<sup>⊥</sup>Department of Bioinspired Science, Ewha Womans University, Seoul 120-750, Korea

## S Supporting Information

**ABSTRACT:** Light-harvesting subphthalocyanine–ferrocenophane (SubPc–Fc; **1**) and subphthalocyanine–naphthalenediimide (SubPc–NDI; **2**) dyads have been synthesized, characterized, and probed by femtosecond laser photolysis. In dyads **1** and **2**, both the electron-donating ferrocenophane and the electron-accepting naphthalenediimide are axially linked with the functional O–Ph groups (at the para position) in the axial positions of SubPc. Electrochemical data show that the SubPcs can act as both electron donors and electron acceptors. The geometric and electronic structures of dyads **1** and **2** were calculated by ab initio B3LYP/6-311G methods. The optimized structures showed that the Fc and NDI entities are separated from SubPc by 8.32 Å (for dyad **1**) and 8.85 Å (For dyad **2**). The distribution of HOMOs and LUMOs suggests the formation of SubPc<sup>•–</sup>–Fc<sup>+</sup> and SubPc<sup>•+</sup>–NDI<sup>•–</sup> as charge-separated states for dyads **1** and **2**, respectively. Upon photoexcitation of the subphthalocyanine unit, these arrays undergo photoinduced electron transfer to form the corresponding charge-separated species, SubPc<sup>•–</sup>–Fc<sup>+</sup> and SubPc<sup>•+</sup>–NDI<sup>•–</sup>, in which SubPc acts as an electron acceptor and an electron donor, respectively, as expected from their redox potentials determined by cyclic voltammetry. Femtosecond transient spectroscopic studies have revealed that a fast charge separation ( $10^{11} \sim 10^{12} \text{ s}^{-1}$ ) occurs for dyads **1** and **2**. From the kinetic studies, the rate of charge recombination and the lifetime of the charge-separated state (SubPc<sup>•+</sup>–NDI<sup>•–</sup>) were found to be  $2.9 \times 10^9 \text{ s}^{-1}$  and 345 ps, respectively.



## INTRODUCTION

Development of relatively simple donor–acceptor models designed to mimic the events of photosynthetic reaction center has been an important goal in science and technology.<sup>1–7</sup> Efficient conversion of light energy into other useful energies requires the effective formation of charge-separated (CS) states that exhibit relatively long lifetimes and high energy contents.<sup>1–7</sup> In the past years, various conjugated macrocycles such as porphyrins, phthalocyanines, and naphthalocyanines were widely employed as building blocks for the photoactive and electroactive assemblies due to their excellent light-harvesting ability in the wide wavelength region (500–700 nm) and to their rich redox chemistry.<sup>8</sup>

Among various planar porphyrinoids used as an antenna, subphthalocyanines (SubPcs)<sup>9</sup> have recently attracted special attention because of their 14  $\pi$ -electron system, cone-shaped aromatic surfaces that show little or no aggregation in solution as established by X-ray analysis,<sup>10</sup> intense absorption and emission in the visible region, and rich electronic properties.<sup>11</sup> These features provide SubPcs with intrinsic chemical and

physical properties and make SubPcs quite different from the higher homologues, phthalocyanines.<sup>12–19</sup> Because of the versatile chemistry of subphthalocyanines,<sup>9</sup> their assemblies for multicomponent photoactive systems are performed via different routes involving peripheral<sup>20</sup> or axial approaches.<sup>10</sup> The advantage of the axial approach is to preserve the electronic characteristics of the macrocycles, since the substitution patterns on the benzene rings remain unaltered. A particular attribute of importance for their application is their ease of oxidation and reduction as compared with other porphyrinoids. Thus, subphthalocyanines have been used as excellent antennas and electron acceptors or donors.<sup>21–23</sup> However, the ability of SubPc acting as both an electron donor and an electron acceptor has yet to be compared using the same linker in the artificial photosynthetic systems.

Received: July 4, 2012

Revised: August 29, 2012

Published: August 30, 2012



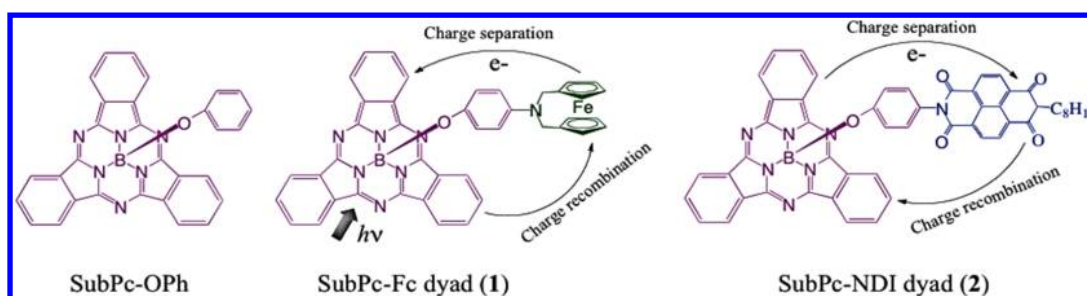
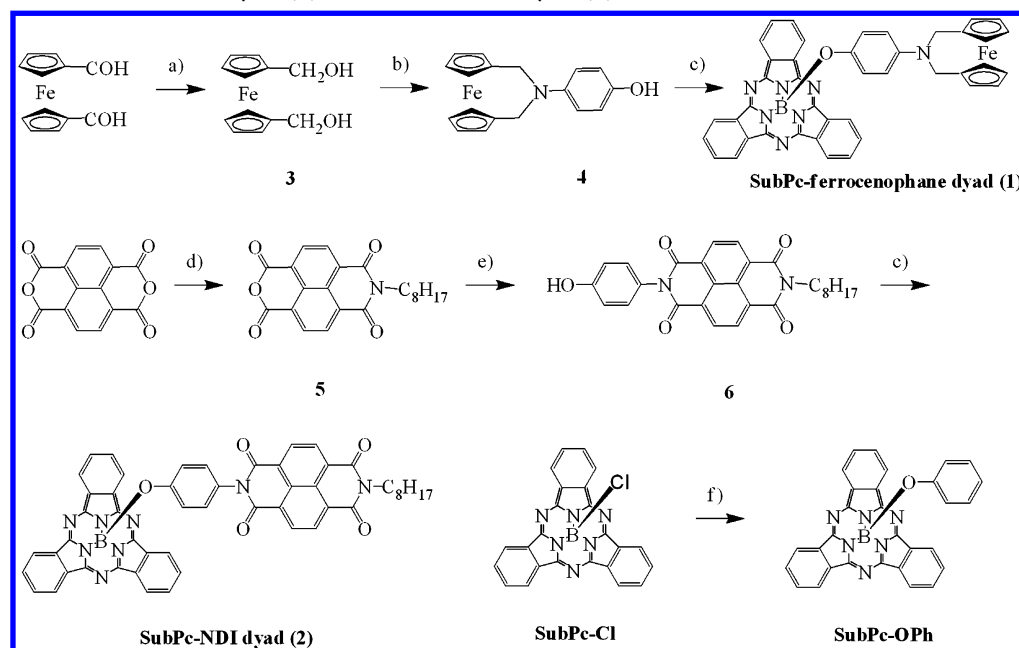


Figure 1. Molecular structures of SubPc–Fc (1), SubPc–NDI (2), and the reference compound, SubPc–OPh.

Scheme 1. Synthesis of SubPc–Fc Dyad (1) and SubPc–NDI Dyad (2)<sup>a</sup>



<sup>a</sup>(a) NaBH<sub>4</sub>, methanol, reflux, 3 h, 96.6%. (b) 4-Aminophenol, RuCl<sub>2</sub>(PPh<sub>3</sub>)<sub>3</sub>, 180 °C, 20 h, 35.0%. (c) SubPc–Cl, toluene, reflux, 16 h, 43.9% for SubPc–ferrocenophane dyad (1), 72 h, 20.0% for SubPc–NDI dyad (2). (d) DMF, reflux, 2 h and then dropping octylamine solution in toluene for 48 h, 35.0%. (e) 4-Aminophenol, zinc acetate, pyridine, reflux, 48 h, 48.0%. (f) Phenol, toluene, reflux, 16 h, 81.2%.

Taking the aforementioned into consideration, we are interested in investigating the performance of SubPc as both electron donor and acceptor when combined with naphthalenediimide (NDI)<sup>15b,24,25</sup> and ferrocenophane (Fc)<sup>26–28</sup> using the same linker in the artificial photosynthetic systems. In this context, subphthalocyanine–ferrocenophane (SubPc–Fc; 1) and subphthalocyanine–naphthalenediimide (SubPc–NDI; 2) dyads were newly synthesized (Figure 1). In the studied dyads, the electron-donating ferrocenophane and the electron-accepting naphthalenediimide are linked at the para position of the functional O–Ph groups, which locate spatially in the axial positions of subphthalocyanine. Both dyads have been investigated electrochemically, computationally, and spectroscopically for the elucidation of photoinduced intramolecular events in polar benzonitrile (PhCN).

## RESULTS AND DISCUSSION

**Synthesis of SubPc–Fc Dyad (1) and SubPc–NDI Dyad (2).** The preparation of SubPc–ferrocenophane dyad (1) and SubPc–NDI dyad (2) was performed by following the steps as depicted in Scheme 1. Every step of the reaction sequence proceeded smoothly and efficiently to give a good or moderate yield of the product (see Experimental Section for

the synthetic details). Commercially available 1,1′-ferrocenedicarboxaldehyde was reduced to the corresponding dialcohol compound 3 in 96.6% yield, and then the subsequent ferrocenophane formation with 4-aminophenol was carried out in the presence of RuCl<sub>2</sub>(PPh<sub>3</sub>)<sub>3</sub> according to the literature procedure<sup>29</sup> to give compound 4 in 35.0% yield. The hydroxy group in compound 4 was reacted with the axial chlorine atom of the SubPc–Cl<sup>30</sup> to produce SubPc–ferrocenophane dyad (1) in 43.9% yield. The reference compound SubPc–OPh was also synthesized by the reaction of SubPc–Cl in 81.2% yield.

SubPc–NDI dyad (2) was synthesized by three-step reactions. Compound 5 was synthesized by reflux of 1,4,5,8-naphthalene-tetracarboxylic dianhydride with octylamine in 35.0% yield. Then, compound 5 was reacted with 4-aminophenol using Zn(OAc)<sub>2</sub> as catalyst to give the naphthalene diimide 6 in 48.0% yield. Finally, the hydroxy group in compound 6 was reacted with the axial chlorine atom of SubPc–Cl<sup>30</sup> to give SubPc–NDI dyad (2) in 20.0% yield.

SubPc–ferrocenophane dyad (1), SubPc–NDI dyad (2), and their precursor compounds are very soluble in aromatic solvents (i.e., toluene, *o*-dichlorobenzene, and PhCN) and other common organic solvents (i.e., acetone, CH<sub>2</sub>Cl<sub>2</sub>, CHCl<sub>3</sub>,

and THF). The structure and purity of the newly synthesized compounds were confirmed mainly by  $^1\text{H}$  NMR and elemental analysis.  $^1\text{H}$  NMR spectra of **1** and **2** are consistent with the proposed structures, showing the expected features with the correct integration ratios, respectively. The MALDI-TOF mass spectra provided a direct evidence for the structures of **1** and **2**, showing a singly charged molecular ion peak at  $m/z = 714.11$  for **1** and  $m/z = 865.74(M^+ + 1)$  for **2**, respectively. Further confirmation of **1** and **2** was obtained from the steady-state UV/vis measurements as shown in the forthcoming sections.

**Computational Studies of Dyads 1 and 2.** Figure 2 shows the (B3LYP/6-311G)<sup>31</sup> optimized structures of dyads **1**

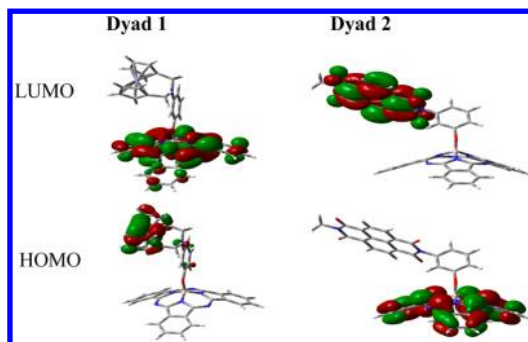


**Figure 2.** Frontier HOMOs and LUMOs of dyads **1** and **2** calculated by the DFT B3LYP/6-311G method.

and **2**. The structures are fully optimized on a Born–Oppenheimer potential energy surface. In the optimized structure of dyad **1**, the Fc and SubPc are connected via short axial linkage making the Fc moiety lie on just the upper position of SubPc, which has a bent structure with upper curvature. The distance between the boron atom of the SubPc and Fc entities is found to be 8.32 Å. The electron distribution of the highest occupied frontier molecular orbitals (HOMO) was found to be entirely located on the Fc entities, while the lowest unoccupied frontier molecular orbital (LUMO) was found to be entirely located over the SubPc entities. This observation suggests the formation of  $\text{SubPc}^{\bullet-}-\text{Fc}^+$  as a charge-separated state.

When turning to dyad **2**, we found that the center-to-center distance between the Boron atom of the SubPc and the NDI entities is separated by 8.85 Å, which is similar to that of dyad **1**

(8.32 Å). The HOMO was found to be entirely located on the SubPc entity, while the LUMO was found to be entirely located over the NDI core. This observation suggests the formation of  $\text{SubPc}^{\bullet+}-\text{NDI}^{\bullet-}$  as charge-separated states.

**Steady-State Absorption and Emission Measurements.** The steady-state absorption spectra of the intense magenta solutions of dyads **1** and **2** and the reference SubPc–OPh are shown in Figure 3. The absorption spectra of the SubPc consist of a high-energy B-band (309 nm) and a lower energy Q-band (566 nm) arising from  $\pi-\pi^*$  transitions associated with 14  $\pi$ -electron systems, analogues to those of porphyrins and phthalocyanines. The absorption spectrum of dyad **1** in the visible region is almost identical to that of SubPc reference taking into account that the absorption of the Fc entity was not observed due to its low molar extinction coefficient. On the other hand, the absorption SubPc–NDI dyad **2** exhibited the characterized absorption bands of SubPc at 565 and 513 nm, as well as the absorption bands of NDI at 340, 357, and 377 nm. These observations suggest that the ground state electronic interactions between SubPc and Fc entities (dyad **1**) and SubPc and NDI entities (dyad **2**) are negligible.

Photophysical behavior was at first investigated by steady-state fluorescence using 570 nm light excitation, which selectively excited the SubPc moiety. As shown in Figure 4,

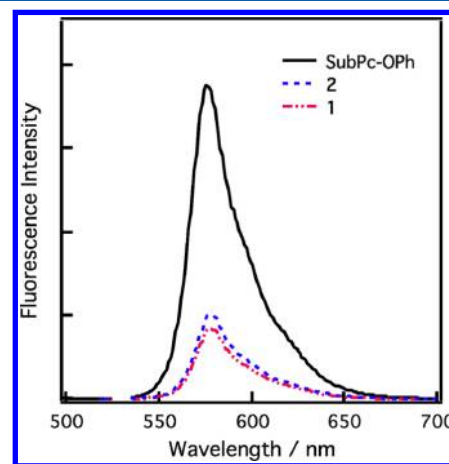


**Figure 4.** Fluorescence spectra of dyads **1** and **2**, as well as the reference SubPc–OPh in PhCN;  $\lambda_{\text{ex}} = 570$  nm.

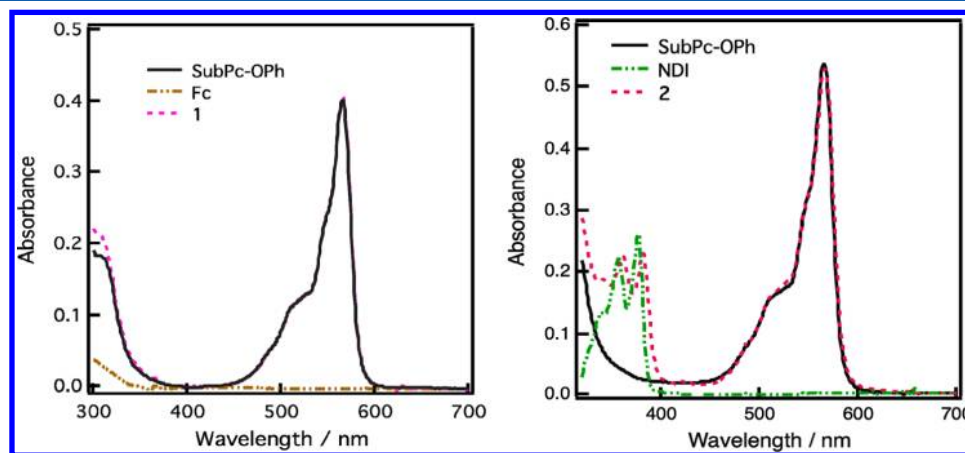


**Figure 3.** Normalized (to the Q-band) absorption spectra of SubPc–Fc (**1**) and SubPc–NDI (**2**), as well as the references SubPc–OPh, NDI, and Fc in PhCN.



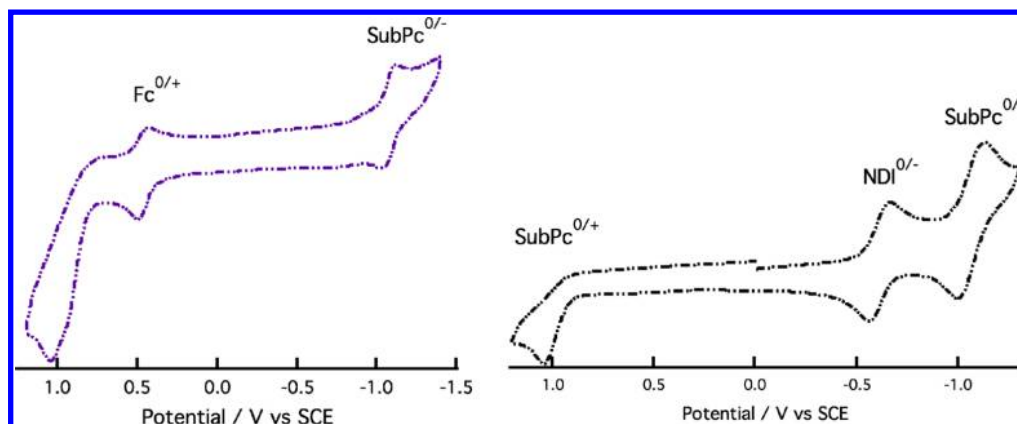


Figure 5. Cyclic voltammograms of dyads 1 (left) and 2 (right) in PhCN. Scan rate = 20 mV/s.

the fluorescence spectrum of SubPc–OPh reference in PhCN shows a maximum at 578 nm (2.15 eV) with fluorescence quantum yield of 0.14. By the axial linkage of SubPc with Fc (dyad 1) and NDI (dyad 2), the emission intensities of the singlet SubPc decreased very much (77% in dyad 1 and 71% in dyad 2) without appreciable shift of the emission peak in PhCN. The fluorescence quantum yields of dyads 1 and 2 were found to be  $3.0 \times 10^{-2}$  and  $4.0 \times 10^{-2}$ , respectively. The efficient fluorescence quenching of SubPc in dyads 1 and 2 suggests that the SubPc can accept an electron from the attached Fc (dyad 1) and can also donate an electron to the attached NDI (dyad 2).

#### Electrochemistry and Energy Levels of Dyads 1 and 2.

In order to establish the energy levels in PhCN, electrochemical studies of the examined dyads and the reference compounds using both cyclic and differential pulse voltammetry (DPV) were performed (Figures 5 and S1). Cyclic voltammograms of SubPc–Fc dyad (1) in PhCN containing  $(n\text{-C}_4\text{H}_9)_4\text{NClO}_4$  as a supporting electrolyte exhibited the first oxidation potential ( $E_{\text{ox}}$ ) of the Fc entity at 0.49 V vs SCE,<sup>32</sup> while the first reduction potential of SubPc was at  $-1.06$  V vs SCE. In the case of dyad 2, the SubPc entity revealed the first  $E_{\text{ox}}$  at 0.95 V vs SCE, while the first  $E_{\text{red}}$  of the NDI entity was at  $-0.59$  V vs SCE.<sup>15b,32</sup>

The driving forces of charge recombination ( $-\Delta G_{\text{CR}}$ ) processes were calculated as 1.55 and 1.54 eV for dyads 1 and 2, respectively.<sup>33</sup> By comparison of these energy levels of the charge-separated states with the energy level of the singlet excited state of SubPc (2.15 eV), the driving forces of charge separation ( $-\Delta G_{\text{CS}}$ ) were estimated as 0.60 and 0.61 eV for dyads 1 and 2, respectively. In addition, the  $-\Delta G_{\text{CS}}$  value from SubPc to the singlet NDI of dyad 2 was found to be 1.68 eV, taking into account the energy of the singlet NDI (3.22 eV). The negative  $\Delta G_{\text{CS}}$  values of  $\text{Fc}^+-\text{SubPc}^{\bullet-}$  and  $\text{SubPc}^{\bullet+}-\text{NDI}^{\bullet-}$  suggest exothermic charge separation via the singlet excited state of SubPc.

**Photodynamics of Dyad 1.** Femtosecond transient absorption spectroscopy was used to obtain further insight into the excited state interactions in SubPc–Fc (1) to corroborate the proposed electron-transfer process. Toward this end, dyad 1 was probed with 440 nm laser light to selectively excite the SubPc fluorophore. The femtosecond transient absorption spectra of SubPc in PhCN (Figure 6) revealed the instantaneous formation of the SubPc–OPh singlet excited state features. Here, the transient absorption spectra are dominated by pronounced bleaching in the visible

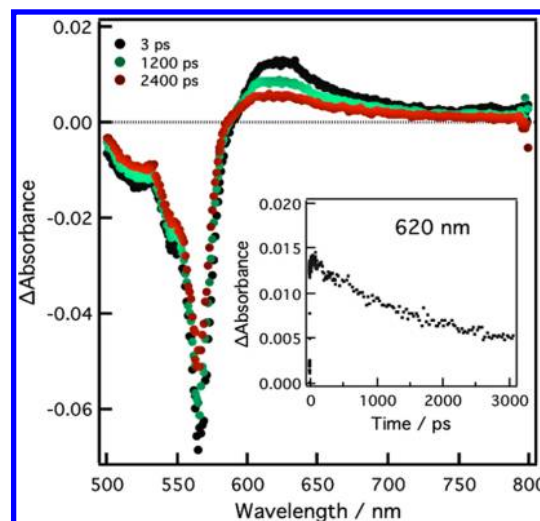
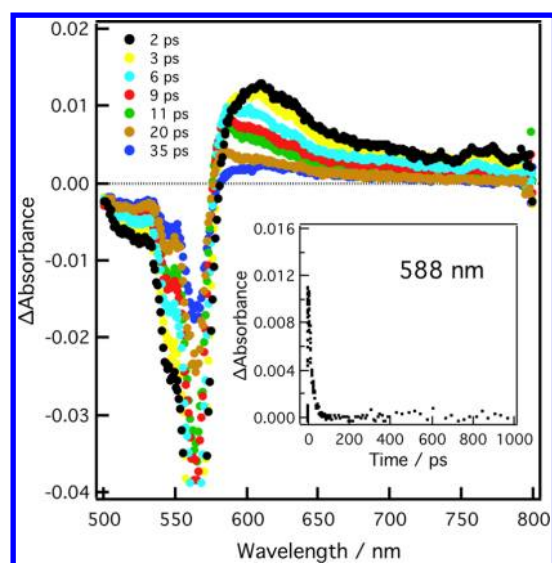


Figure 6. Differential absorption spectra obtained upon femtosecond flash photolysis (440 nm) of SubPc–OPh reference compound in PhCN at the indicated time intervals. Inset: Decay profile of the singlet SubPc at 620 nm, monitoring the intersystem-crossing dynamics.

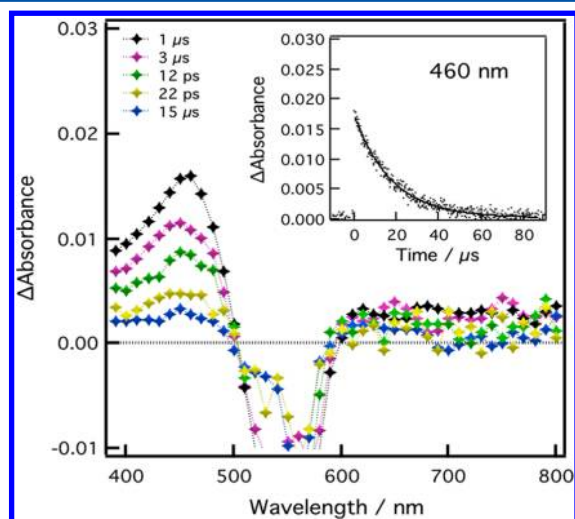
region with a maximum at 564 nm, which is due to depletion of the singlet ground state. SubPc singlet excited state features are relatively long-lived (i.e., 1.70 ns). Implicit is a slow intersystem crossing to the corresponding triplet state of SubPc–OPh.

Figure 7 shows the transient spectral response for representative dyad 1. The spectral features in the visible region, which are seen immediately (i.e., 2 ps) upon excitation of dyad 1 in PhCN, are almost the same as those recorded for the SubPc singlet excited state ( $^1\text{SubPc}^*$ ). The absorption of the singlet SubPc–OPh at 564 and 620 nm decayed with a rate constant of  $8.20 \times 10^{10} \text{ s}^{-1}$ , which is much faster than that observed of the SubPc control in PhCN. This observation indicates occurrence of fast and efficient electron transfer from ferrocenophane to the singlet excited state of SubPc in PhCN. The short distance between the Fe atom of ferrocenophane and the B atom of SubPc (8.32 Å) may rationalize the fast charge-separation process from Fc to the singlet excited state SubPc. We could not observe the absorption band of  $\text{Fc}^+$  due to its low molar extinction coefficient ( $\epsilon = 450 \text{ M}^{-1} \text{ cm}^{-1}$  at 617 nm).<sup>34</sup> It should be noted the anticipated weak absorption band of the SubPc radical anion was hidden under the strong bleaching of the  $^1\text{SubPc}^*$ . For these reasons, it was difficult to determine the rates of charge recombination of dyad 1 in an accurate way.



**Figure 7.** Differential absorption spectra obtained upon femtosecond flash photolysis (440 nm) of SubPc–Fc dyad **1** in PhCN at the indicated time intervals. Inset: Decay profile of the singlet SubPc at 588 nm, monitoring charge separation from ferrocenophane to the singlet SubPc.

The complementary nanosecond transient measurements of SubPc–Fc dyad **1** in PhCN with 570 nm laser excitation, which selectively excited the SubPc moiety, exhibited absorption bands in the visible region with maxima around 450 nm and bleaching with a maximum at around 670 nm (Figure 8). These



**Figure 8.** Nanosecond transient absorption spectra of dyad **1** in PhCN;  $\lambda_{\text{ex}}$  = 570 nm.

absorption bands can be assigned to the triplet excited state of SubPc. To confirm this assignment, we recorded the transient spectra of SubPc in PhCN. Upon excitation at 570 nm, the transient absorption spectra of the SubPc reference showed similar features as that of the SubPc–Fc dyad (Figure S2, Supporting Information). The decay rate of  $^3\text{SubPc}^*-\text{Fc}$  was found to be  $7.15 \times 10^4 \text{ s}^{-1}$  in PhCN, which is faster than that of  $^3\text{SubPc}^*$  ( $3.40 \times 10^4 \text{ s}^{-1}$ ), which may be explained by the collisional quenching of triplet SubPc by the low-lying triplet Fc ( $\sim 1 \text{ eV}$ ).<sup>35</sup> Figure 9 shows an energy-level diagram that summarizes the photoinduced intramolecular events of the

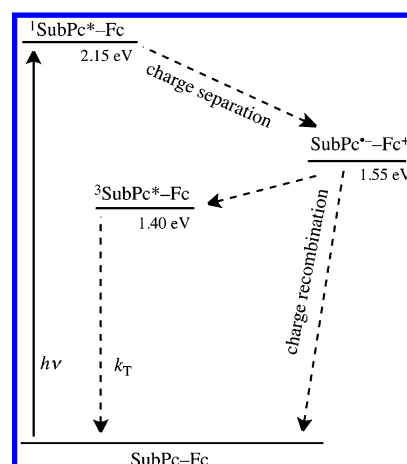


**Figure 9.** Energy-level diagram of dyad **1** in PhCN.

SubPc–Fc dyad in PhCN. Excitation of the SubPc unit of the dyad results in transfer of an electron from the Fc entity to the SubPc entity, which generates the charge-separated state  $\text{SubPc}^{\bullet-}-\text{Fc}^+$  with a rate constant of  $1.34 \times 10^{11} \text{ s}^{-1}$ . The charge-separated state of SubPc–Fc decayed to populate the triplet SubPc, as well as the ground state.

**Photodynamics of Dyad 2.** As shown in Figure 10, the spectrum obtained at 10 ps exhibited the characteristic

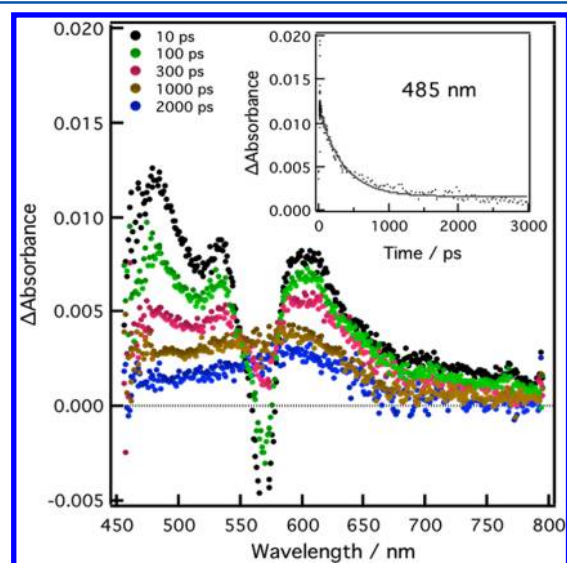


**Figure 10.** Differential absorption spectra obtained upon femtosecond flash photolysis (390 nm) of dyad **2** in PhCN at the indicated time intervals. Inset: Rise–decay profiles of the  $\text{NDI}^{\bullet-}$  at 485 nm, monitoring charge separation and charge recombination from SubPc to NDI.

absorption band due to the NDI radical anion ( $\text{NDI}^{\bullet-}$ ), which is clearly seen at 470, 600, and 700 nm.<sup>15b,32</sup> The characteristic band of the NDI radical anion in the visible region was employed as a reliable probe to determine the rate constants of the charge separation ( $k_{\text{CS}}$ ) and charge recombination ( $k_{\text{CR}}$ ). The time profile was reproduced well by a single-exponential function. From the rise profile of  $\text{NDI}^{\bullet-}$ , the  $k_{\text{CS}}$  was estimated as  $\sim 10^{12} \text{ s}^{-1}$ , which is in a good agreement with the higher driving force for charge separation of  $\text{SubPc}^{\bullet+}-\text{NDI}^{\bullet-}$  via the singlet NDI ( $-\Delta G_{\text{CS}} = 1.68 \text{ eV}$ ). After reaching a peak maximum, the absorbance due to  $\text{NDI}^{\bullet-}$  begins

to decay slowly due to charge recombination. An analysis of the decay profile of the  $\text{NDI}^{\bullet-}$  region yielded a rate constant of  $2.90 \times 10^9 \text{ s}^{-1}$  for the decay of the radical-ion pair, from which the lifetime of the charge-separated state ( $\tau_{\text{CS}}$ ) was determined to be 345 ps. The nanosecond spectra of dyad 2 shown in Figure 11 exhibited the formation of the  $^3\text{SubPc}^*-\text{NDI}$ . This

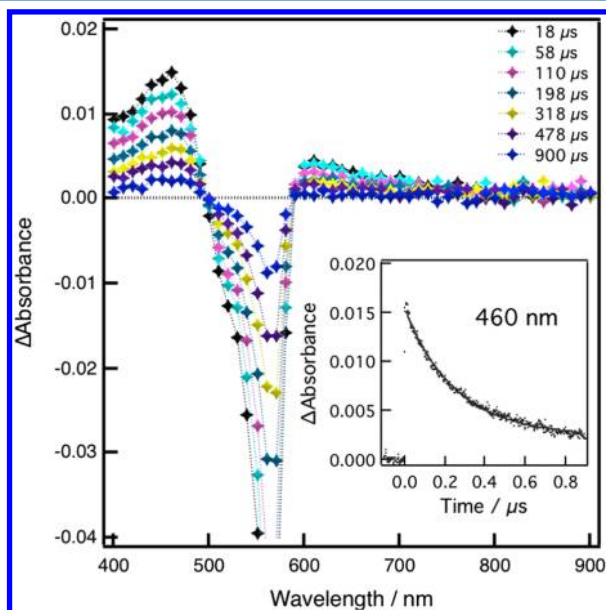


**Figure 11.** Nanosecond transient absorption spectra of dyad 2 in PhCN at the indicated time intervals;  $\lambda_{\text{ex}} = 525 \text{ nm}$ . Inset: Decay profile of the  $^3\text{SubPc}^*$  at 460 nm.

formation of the triplet SubPc is in good agreement with the higher energy level of the charge-separated state (1.54 eV) as compared with the triplet SubPc (1.40 eV). The results of the photochemical properties of dyad 2 are summarized with the help of an energy-level diagram shown in Figure 12.

## CONCLUSION

We reported in this article the electron-donating and electron-accepting properties of the light-harvesting subphthalocyanine by preparing novel artificial photosynthetic subphthalocyanine-ferrocenophane and subphthalocyanine-naphthalenediimide dyads. The redox potentials and site of electron transfer were established from electrochemical studies. Free-energy calculations revealed charge separation from ferrocenophane to the singlet excited SubPc to yield the charge-separated state ( $\text{SubPc}^{\bullet-}-\text{Fc}^+$ ; dyad 1) and from the SubPc to the singlet NDI to yield the charge-separated state ( $\text{SubPc}^{\bullet+}-\text{NDI}^{\bullet-}$ ; dyad 2) to be energetically favorable. Steady-state emission and femtosecond laser flash photolysis studies provided tangible evidence for the occurrence of photoinduced electron transfer in these donor-acceptor systems by providing a spectral signature for  $\text{NDI}^{\bullet-}$  formation in the near-IR region. The kinetics of the charge separation and charge recombination evaluated from femtosecond laser flash photolysis studies revealed fast and efficient charge separation (dyads 1 and 2) and relatively slow charge recombination of dyad 2 (345 ps). Nanosecond transient absorption studies revealed the charge-recombination process to populate the triplet SubPc as well as the SubPc ground state. The present study successfully demonstrates utilization of subphthalocyanine as a suitable candidate to build new types of donor-acceptor dyads for light-energy-harvesting related applications.

## EXPERIMENTAL SECTION

**Materials and Instruments.** Reagents and solvents were purchased as reagent grade and used without further purification.  $\text{SubPc}-\text{Cl}$ ,<sup>30</sup>  $\text{SubPc}-\text{OPh}$ ,<sup>30</sup> and compound 4<sup>29</sup> were synthesized according to the published methods. All reactions were performed using dry glassware under nitrogen atmosphere. Analytical TLC was carried out on Merck 60 F254 silica gel plate, and column chromatography was performed on Merck 60 silica gel (230–400 mesh). Melting points were determined on an Electrothermal IA 9000 series melting point apparatus and are uncorrected. NMR spectra were recorded on

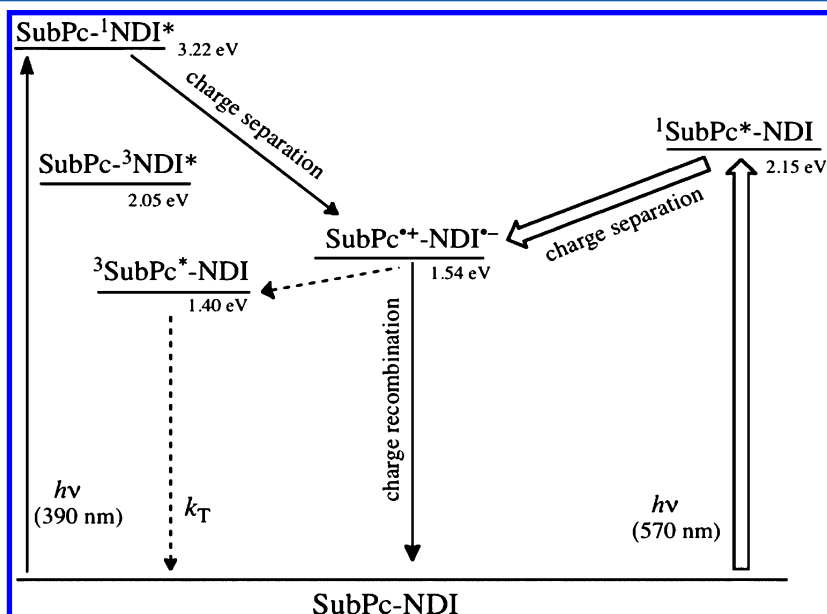


**Figure 12.** Energy-level diagram of SubPc-NDI dyad in deaerated PhCN.



a Varian Mercury-400 (400 MHz) spectrometer with TMS peak as reference. UV/vis spectra were recorded on a Jasco V-550 spectrometer. MALDI-TOF MS spectra were recorded with an Applied Biosystems Voyager-DE-STR. Elemental analyses were performed with a Perkin-Elmer 2400 analyzer.

Steady-state fluorescence spectra were measured on a Shimadzu RF-5300 PC spectrofluorophotometer equipped with a photomultiplier tube having high sensitivity in the 700–800 nm region. Cyclic voltammograms were carried on a BAS CV-50W Voltammetric Analyzer. A platinum disk electrode was used as working electrode, while a platinum wire served as a counter electrode. A SCE electrode was used as a reference electrode. All measurements were carried out in *o*-dichlorobenzene containing tetra-*n*-butylammonium hexafluorophosphate (TBAPF<sub>6</sub>, 0.1 M) as the supporting electrolyte. The scan rate = 20 mV s<sup>-1</sup>. Density-functional theory (DFT) calculations were performed on a COMPAQ\_DS20E computer.

The computational calculations were performed by using DFT B3LYP/6-311G methods with the AUSSIAN 03 software package on high-speed PCs.<sup>36</sup> The frontier HOMO and LUMO were generated by using the Gauss View software program (ver. 3.09) developed by Semichem, Inc.

The studied compounds were excited by a Panther OPO pumped by a Nd:YAG laser (Continuum, SLII-10, 4–6 ns fwhm) at  $\lambda$  = 440 nm with the powers of 1.5 and 3.0 mJ/pulse. The transient absorption measurements were performed using a continuous xenon lamp (150 W) and an InGaAs-PIN photodiode (Hamamatsu 2949) as a probe light and a detector, respectively. The output from the photodiodes and a photomultiplier tube was recorded with a digitizing oscilloscope (Tektronix, TDS3032, 300 MHz). Femtosecond transient absorption spectroscopy experiments were conducted using an ultrafast source, Integra-C (Quantronix Corp.); an optical parametric amplifier, TOPAS (Light Conversion Ltd.); and a commercially available optical detection system, Helios, provided by Ultrafast Systems LLC. The sources for the pump and probe pulses were derived from the fundamental output of Integra-C (780 nm, 2 mJ/pulse and fwhm = 130 fs) at a repetition rate of 1 kHz. Seventy-five percent of the fundamental output of the laser was introduced into TOPAS which has optical frequency mixers resulting in a tunable range from 285 to 1660 nm, while the rest of the output was used for white light generation. Typically, 2500 excitation pulses were averaged for 5 s to obtain the transient spectrum at a set delay time. Kinetic traces at appropriate wavelengths were assembled from the time-resolved spectral data. All measurements were conducted at 298 K. The transient spectra were recorded using fresh solutions in each laser excitation.

**1,1'-Ferrocenedimethanol (3).** To a solution of 1,1'-ferrocenedicarboxaldehyde (0.50 g, 2.06 mmol) in methanol (20 mL) was added sodium borohydride (0.39 g, 10.33 mmol), and the reaction mixture was refluxed for 3 h. The solution was cooled to room temperature and poured into iced water (300 mL). The crude product was extracted with ethyl acetate, the organic layer was dried over Na<sub>2</sub>SO<sub>4</sub>, and the solvent was removed under reduced pressure. The residue was chromatographed on silica gel with ethylacetate/*n*-hexane (1:1) to give compound 3 (0.49 g, 96.6%) as a red solid. Mp 105–107 °C. <sup>1</sup>H NMR (400 MHz, acetone, *d*<sub>6</sub>):  $\delta$  = 4.33 (d, *J* = 6.0 Hz, 4H), 4.16 (m, 4H), 4.09 (m, 4H). Anal. Calcd for C<sub>12</sub>H<sub>14</sub>O<sub>2</sub>Fe: C, 58.57%; H, 5.73%. Found: C, 58.53%; H, 5.78%.

**N-4-(Hydroxyphenyl)-2-aza-[3]-ferrocenophane (4).** To a solution of compound 3 (0.20 g, 0.806 mmol) in 1-

methyl-2-pyrrolidinone (1.5 mL) were added 4-aminophenol (88 mg, 0.806 mmol) and RuCl<sub>2</sub>(PPh<sub>3</sub>)<sub>3</sub> (39 mg, 0.403 mmol), and the mixture was heated to 180 °C and then stirred for 20 h. The solution was cooled to room temperature, and the solvent was removed under reduced pressure. The product was chromatographed on silica gel with dichloromethane/methanol (25:1) to give compound 4 (90 mg, 35.0%) as a yellowish solid. Mp 122–124 °C. <sup>1</sup>H NMR (400 MHz, acetone, *d*<sub>6</sub>):  $\delta$  = 7.65 (br, s, 1H), 6.91 (br, s, 2H), 6.78 (br, s, 2H), 4.17 (br, s, 4H), 4.04 (br, s, 4H), 3.64 (br, s, 4H). Anal. Calcd for C<sub>18</sub>H<sub>17</sub>NOFe: C, 67.73%; H, 5.37%; N, 4.39%. Found: C, 67.69%; H, 5.42%; N, 4.34%.

**SubPc–Ferrocenophane Dyad (1).** Compound 4 (90 mg, 0.28 mmol) was added to a solution of SubPc–Cl (25 mg, 0.058 mmol) in toluene (5 mL), and the solution was refluxed for 16 h. The reaction solution was cooled to room temperature, and the solvent was removed under reduced pressure. The residue was chromatographed on silica gel with dichloromethane/methanol (25:1) to give compound 1 (18 mg, 43.9%) as a purple solid. Mp 147–150 °C. <sup>1</sup>H NMR (400 MHz, CDCl<sub>3</sub>):  $\delta$  = 8.86 (m, 6H), 7.91 (m, 6H), 6.40 (d, *J* = 8.8 Hz, 2H), 5.36 (d, *J* = 8.8 Hz, 2H), 4.07 (s, 8H), 3.56 (s, 4H). UV/vis (toluene):  $\lambda_{\text{max}}$  = 565, 513, and 309 nm. MS (MALDI-TOF): *m/z* for C<sub>42</sub>H<sub>28</sub>BN<sub>7</sub>OFe Calcd. 713.36. Found 714.11(M<sup>+</sup>), 715.15(M<sup>+</sup> + 1), 716.10(M<sup>+</sup> + 2). Anal. Calcd: C, 70.91%; H, 3.68%; N, 13.78%. Found: C, 70.85%; H, 3.72%; N, 13.75%.

**SubPc–OPh.** To a solution of phenol (0.12 g, 1.28 mmol) in toluene (10 mL) was added SubPc–Cl (0.12 g, 0.28 mmol), and the solution was refluxed for 6 h. The reaction mixture was cooled to room temperature, and the solvent was evaporated under reduced pressure. The product was chromatographed on silica gel with dichloromethane/methanol (200:1) to give SubPc–OPh (0.11 g, 81.2%) as a red solid. Mp 138–139 °C. <sup>1</sup>H NMR (400 MHz, CDCl<sub>3</sub>):  $\delta$  = 8.84 (dd, *J* = 9.3 Hz, *J* = 2.7 Hz, 6H), 7.90 (dd, *J* = 9.3 Hz, *J* = 2.7 Hz, 6H), 6.73 (m, 2H), 6.60 (m, 1H), 5.37 (d, *J* = 8.6 Hz, 2H). UV/vis (toluene):  $\lambda_{\text{max}}$  = 302, 524, 562 nm. MS (MALDI-TOF): *m/z* for C<sub>30</sub>H<sub>17</sub>BN<sub>6</sub>O Calcd 488.31. Found 487.45. Anal. Calcd: C, 73.79%; H, 3.51%; N, 17.21%. Found: C, 73.77%; H, 3.55%; N, 17.15%.

**N-Octylnaphthalene-1,8-dicarboxyanhydride-4,5-dicarboximide (5).** 1,4,5,8-Naphthalene-tetracarboxylic dianhydride (5.0 g, 18.6 mmol) was mixed with DMF (100 mL). The mixture was refluxed under N<sub>2</sub> for 2 h, and then octylamine (0.7 g, 2.6 mmol) in toluene (200 mL) was added dropwise to the reaction flask and the solution was refluxed for 48 h. The solvent was stripped under reduced pressure, and the residue was column chromatographed on silica gel with dichloromethane/acetone (30:1) to give compound 5 (0.72 g, 35.0%). Mp 400 °C (dec.). <sup>1</sup>H NMR (400 MHz, CDCl<sub>3</sub>):  $\delta$  = 8.82 (s, 4H), 4.20 (t, 2H), 1.00–1.70 (m, 12H), 0.81 (t, 3H). Anal. Calcd: C, 69.64%; H, 5.58%; N, 3.69%. Found: C, 69.49%; H, 5.69%; N, 3.77%.

**N,N-(4-Hydroxyphenyl)octylnaphthalene-1,8,4,5-bis-(dicarboximide) (6).** Compound 5 (0.5 g, 1.3 mmol) was mixed with 4-aminophenol (0.5 g, 4.6 mmol), zinc acetate (1.0 g, 5.46 mmol), and pyridine (30 mL). The mixture was heated to reflux under N<sub>2</sub> and kept at reflux for 48 h. The solvent was evaporated under reduced pressure. The residue was column chromatographed on silica gel with dichloromethane/acetone (10:1) to afford compound 6 (0.3 g, 48.0%) as a brown solid. Mp. 400 °C. <sup>1</sup>H NMR (400 MHz, CDCl<sub>3</sub>):  $\delta$  = 8.82 (s, 4H), 7.38 (d, *J* = 8.1 Hz, 2H), 7.02 (d, *J* = 8.1 Hz, 2H), 4.20 (t, 2H),



3.72 (s, 1H), 1.02–1.70 (m, 12H), 0.73 (t, 3H). Anal. Calcd: C, 71.47%; H, 5.57%; N, 5.95%. Found: C, 71.34%; H, 5.70%; N, 6.08%.

**SubPc–NDI Dyad (2).** Compound 6 (0.1 g, 0.21 mmol) was added to toluene (20 mL) and stirred under nitrogen for 1 h. To this mixture was added SubPc–Cl (0.1 g, 0.23 mmol). After reflux for 72 h, the mixture was cooled to room temperature, and the solvent was evaporated. The crude product was chromatographed on silica gel with dichloromethane/methanol (40:1) to produce SubPc–NDI dyad (2) (36 mg, 20.0%) as a purple solid. Mp. >360 °C (dec.).  $^1\text{H}$  NMR (400 MHz, DMSO- $d_6$ ):  $\delta$  = 8.92 (dd, 6H), 8.74 (d,  $J$  = 7.1 Hz, 2H), 8.70 (d,  $J$  = 7.1 Hz, 2H), 7.97 (dd, 6H), 6.68 (d,  $J$  = 8.0 Hz, 2H), 5.50 (d,  $J$  = 8.2 Hz, 2H), 4.20 (t, 2H), 1.10–1.71 (m, 12H), 0.81 (t, 3H). MS (MALDI-TOF):  $m/z$  for  $\text{C}_{52}\text{H}_{37}\text{BN}_5\text{O}_5$  Calcd 864.701. Found 865.74 ( $\text{M}^+ + 1$ ). Anal. Calcd: C, 72.23%; H, 4.31%; N, 12.96%. Found: C, 72.12%; H, 4.39%; N, 13.19%. FT-IR (KBr):  $\nu$  = 2954, 2925, 2852, 1705, 1662, 1349, 1245  $\text{cm}^{-1}$ .

## ■ ASSOCIATED CONTENT

### ● Supporting Information

DPV of dyad 2 (Figure S1) and nanosecond spectra of SubPc–OPh control compound (Figure S2). This material is available free of charge via the Internet at <http://pubs.acs.org>.

## ■ AUTHOR INFORMATION

### Corresponding Author

\* E-mail: mohamedelkhouly@yahoo.com (M.E.K.); kykay@ajou.ac.kr (K.-Y.K.); fukuzumi@chem.eng.osaka-u.ac.jp (S.F.).

### Notes

The authors declare no competing financial interest.

## ■ ACKNOWLEDGMENTS

This research was supported by Grants-in-Aid (No. 20108010) from the Ministry of Education, Culture, Sports, Science and Technology, Japan, and KOSEF/MEST through the WCU project (R31-2008-000-10010-0) of Korea.

## ■ REFERENCES

- (1) (a) Gust, D.; Moore, T. A.; Moore, A. L. *Acc. Chem. Res.* **2001**, *34*, 40–48. (b) Gust, D.; Moore, T. A.; Moore, A. L. *Acc. Chem. Res.* **2009**, *42*, 1890–1898.
- (2) (a) Wasielewski, M. R. *Chem. Rev.* **1992**, *92*, 435–461. (b) Wasielewski, M. R. *J. Org. Chem.* **2006**, *71*, 5051–5066. (c) Wasielewski, M. R. *Acc. Chem. Res.* **2009**, *42*, 1910–1921.
- (3) (a) Fukuzumi, S. *Org. Biomol. Chem.* **2003**, *1*, 609–620. (b) Fukuzumi, S. *Phys. Chem. Chem. Phys.* **2008**, *10*, 2283–2297. (c) Fukuzumi, S.; Kojima, T. *J. Mater. Chem.* **2008**, *18*, 1427–1439. (d) Fukuzumi, S. *Bull. Chem. Soc. Jpn.* **2006**, *79*, 177–195. (e) Fukuzumi, S.; Honda, T.; Ohkubo, K.; Kojima, T. *Dalton Trans.* **2009**, 3880–3889. (f) Fukuzumi, S.; Ohkubo, K. *J. Mater. Chem.* **2012**, *22*, 4575–4587.
- (4) (a) de la Torre, G.; Vázquez, P.; Agullo-Lopez, F.; Torres, T. *Chem. Rev.* **2004**, *104*, 3723–3750. (b) Bottari, G.; de la Torre, G.; Guldi, D. M.; Torres, T. *Chem. Rev.* **2010**, *110*, 6768–6816. (c) Guldi, D. M.; Rahman, G. M. A.; Sgobba, V.; Ehli, C. *Chem. Soc. Rev.* **2006**, *35*, 471–487.
- (5) (a) Ohkubo, K.; Kotani, H.; Shao, J.; Ou, Z.; Kadish, K. M.; Li, G.; Pandey, R. K.; Fujitsuka, M.; Ito, O.; Imahori, H.; Fukuzumi, S. *Angew. Chem., Int. Ed.* **2004**, *43*, 853–856. (b) Fukuzumi, S.; Ohkubo, K.; E, W.; Ou, Z.; Shao, J.; Kadish, K. M.; Hutchison, J. A.; Ghiggino, K. P.; Sinti, P. J.; Crossley, M. J. *J. Am. Chem. Soc.* **2003**, *125*, 14984–14985. (c) Fukuzumi, S.; Ohkubo, K.; Imahori, H.; Shao, J.; Ou, Z.;

Zheng, G.; Chen, Y.; Pandey, R. K.; Fujitsuka, M.; Ito, O.; Kadish, K. M. *J. Am. Chem. Soc.* **2001**, *123*, 10676–10683.

(6) (a) Tanaka, M.; Ohkubo, K.; Gros, C. P.; Guillard, R.; Fukuzumi, S. *J. Am. Chem. Soc.* **2006**, *128*, 14625–14633. (b) Takai, A.; Chkounda, M.; Eggenspieler, A.; Gros, C. P.; Lachkar, M.; Barbe, J.-M.; Fukuzumi, S. *J. Am. Chem. Soc.* **2010**, *132*, 4477–4489.

(7) (a) Fukuzumi, S.; Kotani, H.; Ohkubo, K.; Ogo, S.; Tkachenko, N. V.; Lemmetyinen, H. *J. Am. Chem. Soc.* **2004**, *126*, 1600–1601. (b) Murakami, M.; Ohkubo, K.; Fukuzumi, S. *Chem.–Eur. J.* **2010**, *16*, 7820–7832. (c) Hoshino, M.; Uekusa, H.; Tomita, A.; Koshihara, S.; Sato, T.; Nozawa, S.; Adachi, S.; Ohkubo, K.; Kotani, H.; Fukuzumi, S. *J. Am. Chem. Soc.* **2012**, *134*, 4569–4572.

(8) (a) *Phthalocyanines: Properties and Applications*; Leznoff, C. C., Lever, A. B. P., Eds.; VCH: Weinheim, Germany, 1996; Vol. 4. (b) El-Khouly, M. E.; Kang, E. S.; Kay, K.-Y.; Choi, C. S.; Araki, Y.; Ito, O. *Chem.–Eur. J.* **2007**, *13*, 2854–2863. (c) El-Khouly, M. E.; Kim, J. H.; Kay, K.-Y.; Choi, C. S.; Ito, O.; Fukuzumi, F. *Chem.–Eur. J.* **2009**, *15*, 5301–5310. (d) Liu, J.-Y.; El-Khouly, M. E.; Fukuzumi, S.; Ng, D. K. P. *Chem.–Eur. J.* **2011**, *17*, 1605–1613. (e) D'Souza, F.; Maligaspe, E.; Ohkubo, K.; Zandler, M. E.; Subbaiyan, N. K.; Fukuzumi, S. *J. Am. Chem. Soc.* **2009**, *131*, 8787–8797.

(9) Claessens, C. G.; González-Rodríguez, D.; Torres, T. *Chem. Rev.* **2002**, *102*, 835–854.

(10) (a) Kietai, H. *Monatsh. Chem.* **1974**, *105*, 405–418. (b) Rauschnabel, J.; Hanack, M. *Tetrahedron Lett.* **1995**, *36*, 1629–1632. (c) Kasuga, K.; Idehara, T.; Handa, M.; Ueda, Y.; Fujiwara, T.; Isa, K. *Bull. Chem. Soc. Jpn.* **1996**, *69*, 2559–2563.

(11) (a) del Rey, B.; Keller, U.; Torres, T.; Rojo, G.; Agulló-López, F.; Nonell, S.; Martí, C.; Brasselet, S.; Ledoux, I.; Zyss, J. *J. Am. Chem. Soc.* **1998**, *120*, 12808–12817. (b) Aminur Rahman, G. M.; Lüders, D.; Rodríguez-Morgade, S.; Caballero, E.; Torres, T.; Guldi, D. M. *ChemSusChem* **2009**, *2*, 330–335.

(12) (a) El-Khouly, M. E.; Araki, Y.; Ito, O.; Gadde, S.; Zandler, M. E.; D'Souza, F. *J. Porphyrins Phthalocyanines* **2006**, *10*, 1156–1164. (b) El-Khouly, M. E.; Ju, D. K.; Kay, K.-Y.; D'Souza, F.; Fukuzumi, S. *Chem.–Eur. J.* **2010**, *16*, 6193–6202.

(13) (a) Verreest, B.; Rand, B. P.; Cheyng, D.; Hadipour, A.; Aernouts, T.; Heremans, P.; Medina, A.; Claessens, C. G.; Torres, T. *Adv. Energy Mater.* **2011**, *1*, 565–568. (b) Luhman, W. A.; Holmes, R. J. *Adv. Funct. Mater.* **2011**, *21*, 764–771. (c) Shimizu, S.; Nakano, S.; Hosoya, T.; Kobayashi, N. *Chem. Commun.* **2011**, *47*, 316–318. (d) Gonzalez-Rodríguez, D.; Carbonell, E.; Guldi, D. M.; Torres, T. *Angew. Chem., Int. Ed.* **2009**, *48*, 8032–8036.

(14) (a) Solntsev, P. V.; Spurgin, K. L.; Sabin, J. R.; Heikal, A. A.; Nemykin, V. N. *Inorg. Chem.* **2012**, *51*, 6537–6547. (b) Gonzalez-Rodríguez, D.; Bottari, G. *J. Porphyrins Phthalocyanines* **2009**, *13*, 624–636. (c) Brothers, P. J. *Chem. Commun.* **2008**, 2090–2102.

(15) (a) El-Khouly, M. E.; Gutierrez, A. M.; Sastre-Santos, A.; Fernandez-Lazaro, F.; Fukuzumi, S. *Phys. Chem. Chem. Phys.* **2012**, *14*, 3612–3621. (b) El-Khouly, M. E.; Moiseev, A. G.; van der Est, A.; Fukuzumi, S. *ChemPhysChem* **2012**, *13*, 1191–1198.

(16) (a) Torres, T. *Angew. Chem., Int. Ed.* **2006**, *45*, 2834–2837. (b) Sastre, A.; Torres, T.; Diaz-Garcia, M. A.; Agulló-López, F.; Dhenaut, C.; Brasselet, S.; Ledoux, I.; Zyss, J. *J. Am. Chem. Soc.* **1996**, *118*, 2746–2747.

(17) (a) De la Torre, G.; Torres, T.; Agulló-López, F. *Adv. Mater.* **1997**, *9*, 265–269. (b) Kobayashi, N.; Ishizaki, T.; Ishii, K.; Konami, H. *J. Am. Chem. Soc.* **1999**, *121*, 9096–9097.

(18) (a) Kang, S. H.; Kang, Y. S.; Zin, W. C.; Olbrechts, G.; Wostyn, K.; Clays, K.; Persoons, A.; Kim, K. *Chem. Commun.* **1999**, 1661–1662. (b) Claessens, C. G.; Torres, T. *Tetrahedron Lett.* **2000**, *41*, 6361–6365. (c) Kobayashi, N. *Bull. Chem. Soc. Jpn.* **2002**, *75*, 1–19.

(19) (a) Hanack, M.; Heckman, H.; Polley, R. In *Methods in Organic Chemistry*; Schauman, E., Ed.; Georg Thieme Verlag: Stuttgart, Germany, 1998; Vol. E 94, p 717. (b) de la Torre, G.; Nicolau, M.; Torres, T. In *Phthalocyanines: Syntheses, Supramolecular Organization and Physical Properties (Supramolecular Photosensitive and Electroactive Materials)*; Nalwa, H. S., Ed.; Academic Press: New York, 2001; pp 1–111.

- (20) (a) del Rey, B.; Torres, T. *Tetrahedron Lett.* **1997**, 38, 5351–5354. (b) Claessens, C. G.; Torres, T. *J. Am. Chem. Soc.* **2002**, 124, 14522–14523.
- (21) (a) Geyer, M.; Plenzig, F.; Rauschnabel, J.; Hanack, M.; del Rey, B.; Sastre, A.; Torres, T. *Synthesis* **1996**, 1139–1151. (b) Remero-Nieto, C.; Medina, A.; Molina-Ontoria, A.; Claessens, C. C.; Echegoyen, L.; Martin, N.; Torres, T.; Guldi, D. M. *Chem. Commun.* **2012**, 48, 4953–4955.
- (22) (a) González-Rodríguez, D.; Torres, T.; Guldi, D. M.; Rivera, J.; Echegoyen, L. *Org. Lett.* **2002**, 4, 335–338. (b) González-Rodríguez, D.; Torres, T.; Olmstead, M. M.; Rivera, J.; Herranz, M. Á.; Echegoyen, L.; Atienza Castellanos, C.; Guldi, D. M. *J. Am. Chem. Soc.* **2006**, 128, 10680–10681. (c) Romero-Nieto, C.; Guilleme, J.; Villegas, C.; Delgado, J. L.; González-Rodríguez, D.; Martin, N.; Torres, T.; Guldi, D. M. *J. Mater. Chem.* **2011**, 21, 15914–15918.
- (23) (a) El-Khouly, M. E.; Shim, S. H.; Araki, Y.; Ito, O.; Kay, K.-Y. *J. Phys. Chem. B* **2008**, 112, 3910–3917. (b) Kim, J.-H.; El-Khouly, M. E.; Araki, Y.; Ito, O.; Kay, K.-Y. *Chem. Lett.* **2008**, 37, 544–545. (c) El-Khouly, M. E.; Ryu, J. B.; Kay, K.-Y.; Ito, O.; Fukuzumi, S. *J. Phys. Chem. C* **2009**, 113, 15444–15453. (d) El-Khouly, M. E. *Phys. Chem. Chem. Phys.* **2010**, 12, 12746–12752.
- (24) (a) Katz, H. E.; Lovinger, A. J.; Kloc, C.; Siegrist, T.; Li, W.; Lin, Y.-Y.; Dodabalapur, A. *Nature* **2000**, 404, 478–481. (b) Sakai, N.; Mareda, J.; Vauthey, E.; Matile, S. *Chem. Commun.* **2010**, 46, 4225–4237. (c) Fallon, G. D.; Lee, M. A.-P.; Langford, S. J.; Nichols, P. J. *Org. Lett.* **2004**, 6, 655–658. (d) Hansen, J. G.; Feeder, N.; Hailton, D. G.; Gunter, M. J.; Becher, J.; Sanders, J. K. M. *Org. Lett.* **2000**, 2, 449–452.
- (25) (a) Amabilino, D. B.; Stoddart, J. F. *Chem. Rev.* **1995**, 95, 2725–2828. (b) Vicić, D. A.; Odom, D. T.; Nunez, M. E.; Gianolio, D. A.; McLaughlin, L. W.; Barton, J. K. *J. Am. Chem. Soc.* **2000**, 122, 8603–8611. (c) Lee, H. N.; Xu, Z.; Kim, S. K.; Swamy, K. M. K.; Kim, Y.; Kim, S.-J.; Yoon, J. *J. Am. Chem. Soc.* **2007**, 129, 3828–3829. (d) Bhosale, S. V.; Jani, C. H.; Langford, S. J. *Chem. Rev.* **2008**, 37, 331–342.
- (26) (a) Kealy, T. J.; Pauson, P. L. *Nature* **1951**, 168, 1039–1040. (b) Dunitz, J. D.; Orgel, L. E. *Nature* **1953**, 171, 121–122. (c) Woodward, R. B.; Rosenblum, M.; Whiting, M. C. *J. Am. Chem. Soc.* **1952**, 74, 3458–3459. (d) Plesske, K. *Angew. Chem., Int. Ed. Engl.* **1962**, 1, 394–399.
- (27) (a) Manners, I. *Adv. Organomet. Chem.* **1995**, 37, 131–168. (b) Barlow, S.; O'Hare, D. *Chem. Rev.* **1997**, 97, 637–670. (c) Crooks, R. M.; Ricco, A. J. *Acc. Chem. Res.* **1998**, 31, 219–227.
- (28) (a) Marder, S. R.; Perry, J. W. *Science* **1994**, 263, 1706–1707. (b) Patil, A. O.; Heeger, A. J.; Wudl, F. *Chem. Rev.* **1988**, 88, 183–200. (c) Marks, T. J. *Science* **1985**, 227, 881–889. (d) Heo, R. W.; Lee, T. R. *J. Organomet. Chem.* **1999**, 578, 31–42.
- (29) (a) Yamaguchi, I.; Sakano, T.; Ishii, H.; Osakada, K.; Yamamoto, T. *J. Organomet. Chem.* **1999**, 584, 213–216. (b) Sakano, T.; Horie, M.; Osakada, K.; Nakao, H. *Bull. Chem. Soc. Jpn.* **2001**, 74, 2059–2065. (c) Osakada, K.; Sakano, T.; Horie, M.; Suzuki, Y. *Coord. Chem. Rev.* **2006**, 250, 1012–1022.
- (30) Claessens, C. G.; Gonzalez-Rodriguez, D.; Rey, B. D.; Torres, T.; Mark, G.; Schuchmann, H.-P.; Sonntag, C. V.; MacDonald, J. G.; Nohr, R. S. *Eur. J. Org. Chem.* **2003**, 2547–2551.
- (31) (a) *Gaussian 03*; Gaussian, Inc.: Pittsburgh PA, 2003. (b) Yang, Y. *Polyhedron* **2012**, 42, 249–257. (c) Sordo, T.; Menendez, M. *J. Org. Chem.* **2010**, 75, 5904–5910.
- (32) Supur, M.; El-Khouly, M. E.; Seok, J. H.; Kay, K.-Y.; Fukuzumi, S. *J. Phys. Chem. A* **2011**, 115, 14430–14437.
- (33) The driving forces of charge-recombination ( $\Delta G_{CR}$ ) and charge-separation ( $\Delta G_{CS}$ ) processes were calculated by the following equations:  $\Delta G_{CR} = -e(E_{ox} - E_{red})$  and  $\Delta G_{CS} = -\Delta E_{0-0} - (\Delta G_{CR})$  where  $E_{ox}$  is the first oxidation potentials of the electron donors,  $E_{red}$  is the first reduction potentials of the electron acceptors, and  $\Delta E_{0-0}$  is the energy of the 0–0 transition energy gap between the lowest excited state and the ground state of SubPc (2.15 eV) and NDI (3.22 eV). The negligible value of the static Coulombic energy in polar PhCN was not considered in the calculations of  $\Delta G_{CR}$ .
- (34) (a) Fery-Forgues, S.; Delavaux-Nicot, B. *J. Photochem. Photobiol., A* **2000**, 132, 137–159. (b) Fukuzumi, S.; Okamoto, K.; Gros, C. P.; Guillard, R. *J. Am. Chem. Soc.* **2004**, 126, 10441–10449.
- (35) Araki, Y.; Yasumura, Y.; Ito, O. *J. Phys. Chem. B* **2005**, 109, 9843–9848.
- (36) For a general review on DFT applications of donor–acceptor systems, see: Zandler, M. E.; D'Souza, F. C. R. *Chem.* **2006**, 9, 960–981.